Well-Defined PMMA Brush on Silica Particles Fabricated by Surface-Initiated Photopolymerization (SIPP)

Fengting Chen,[†] Xuesong Jiang,*[,†] Rui Liu,[‡] and Jie Yin*[,†]

School of Chemistry & Chemical Technology, State Key Laboratory of Metal Matrix Composites, Shanghai Jiao Tong University, and National Engineering Research Center for Nanotechnology, Shanghai 200240, People's Republic of China

ABSTRACT The photochemical method is a convenient and simple way to synthesize the polymer brush on surface. We presented here a facile approach to fabricate PMMA brush on silica particles (SPs) by combination of self-assembly monolayer of hyperbranched polymeric thioxanthone (HPTX) and surface-initiated photopolymerization (SIPP). HPTX was immobilized on the surface of silica particles (SPs) through nucleophilic addition between amine and epoxy groups, and then initiated photopolymerization of MMA to generate PMMA brush on SPs at room temperature. The whole process was well-traced by FT-IR, TGA, SEM, and TEM. The results show that it is easy to create PMMA brushes of tunable thickness under UV irradiation. Especially, TEM images reveal the obvious formation of well-defined hybrid particles with SPs as the core and PMMA layers as the shell. The obtained hybrid particles can be implanted into PMMA matrix to produce PMMA composite with enhanced thermal and mechanical properties.

KEYWORDS: PMMA brush • surface-initiated photopolymerization • hybrid particles

INTRODUCTION

The surface modified with thin polymer brush is of great interest (1−6) because of its potential applications in many surface-based technologies such as composite materials, biomaterials, adhesion and wetting, molecular recognition, microfluidics, chemical sensing, and organic synthesis (7−13). Generally, a polymer brush can be prepared by physisorption and covalent attachment accomplished by either "grafting to" or "grafting from" approaches. Compared to methods of physisorption and "grafting to", a surface-initiated polymerization (SIP, "grafting from") approach, based on initiators being bound to a surface to initiate polymerization, is a powerful alternative to control the thickness, functionality, and density of polymer brushes with molecular precision (14−16). Quite a few methods of SIP have been used to fabricate polymer brushes on a variety of substrates, especially photopolymerization (17−19) and controlled polymerization such as ATRP (20−22), RAFT (23, 24), ROMP (25), and ROP (26). Among various polymerizations, free-radical photopolymerization is a most convenient and simple way and provides distinct advantages, such as resistance to moisture, a wide application in variety of organic functional groups (27), low cost of operation, and temperature independence (28−30).

To the best of our knowledge, there are only a few studies on surface-initiated photopolymerization (SIPP) on the surface of particles. Tsubokawa and co-workers have investigated the photograft polymerization of various vinyl monomers initiated by eosin moieties immobilized on a nanosized silica surface in the presence of a reducing agent and oxygen at room temperature in water (31). Similarly, preparation of polymeric core−shell and multilayer nanoparticles based on surface-initiated polymerization using in situ synthesized photoiniferters was reported by Mayes et al. (32). The photochemical methods to fabricate a well-defined polymer brush with high density on the surface of the substrate include two important prerequisites: the proper choice of photoinitiators and immobilization of photoinitiator onto the surface of the substrate (33). As we all know, the most widely used initiators in photochemical synthesis of polymer brushes are derivatives of 2,2-azobis-(isobutyronitrile) (AIBN) (34, 35). However, AIBN has been proven to be sensitive to heat and to have a relatively low absorbency at 365 nm, the irradiation wavelength most widely utilized for photopolymerization (36, 37). Therefore, immobilization of photoinitiators with high performance onto the surface of the substrate becomes the key step in surface-initiated photopolymerization. On the basis of immobilization of dendritic thioxanthone photoinitiators (DAB-16-TX or DAB-64-TX) containing a co-initiator amine group onto the surface of silicon wafer, we previously developed a novel photochemical approach to fabricate polymer brush on planar surface (38, 39). In this text, we tried to synthesize polymer brush on SPs through the same photochemical approach. Because of the shield of light caused by particles (diameter >100 nm), it is a challenge to synthesize polymer brush on particles by photochemical approach. Because of the excellent UV absorbance at 365−400 nm (39, 40), thioxanthone can well-absorb UV light even in the case of pigment particles' shield and is consequently widely used in photocuring systems containing

* Corresponding author. Tel.: +86-21-54743268. Fax: +86-21-54747445. E-mail: ponygle@sjtu.edu.cn (X.J.); jyin@sjtu.edu.cn (J.Y.).
Received for review November 06, 2009 and accepted March 10, 2010
[†] Shanghai Jiao Tong University.
[‡] National Engineering Research Center for Nanotechnology.
DOI: 10.1021/am900758j

Scheme 1

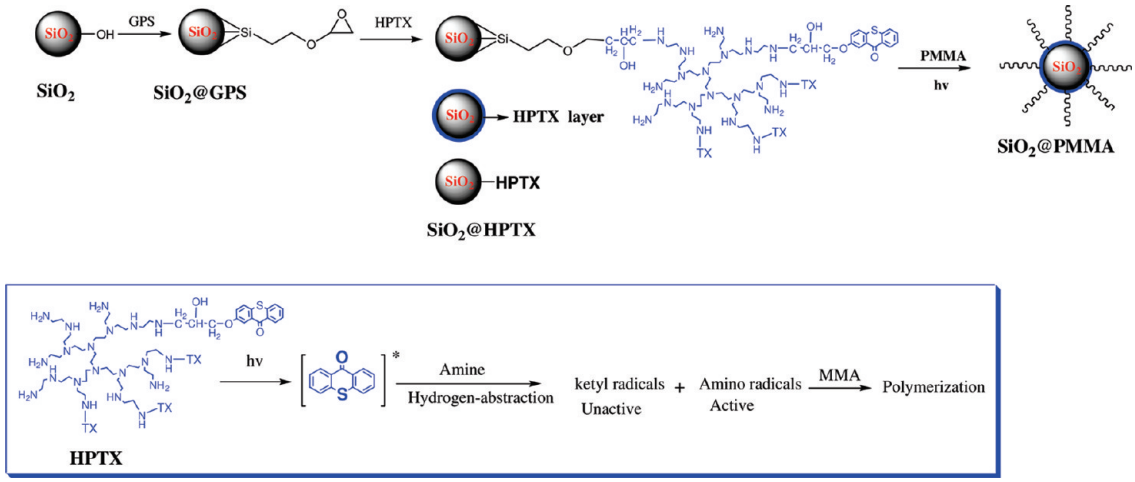

pigment particles such as coating and printing ink (41−43). It is these characterizations to motivate us to immobilize TX photoinitiator on the surface of SPs to synthesize polymer brushes by a photochemical approach. The whole strategy is illustrated in Scheme 1. Through introduction of epoxy groups to the surface of SPs in the first step, the hyperbranched polymeric thioxanthone photoinitiator (HPTX) can be easily rooted on the surface by a covalent bond. The amine groups are just like a lot of anchors that can react with epoxy groups through nucleophilic addition. The PMMA brush on the surface of SPs was the prepared by surface-initiated photopolymerization to generate organic/inorganic hybrid particles with SPs as the core and PMMA layers as the shell. The whole processes of synthesis were well-traced by FT-IR, TGA, SEM, and TEM. Then the obtained SiO_2@PMMA hybrid particles were further implanted into the PMMA matrix to enhance the properties of PMMA films.

EXPERIMENTAL SECTION

Materials. 3-Glycidoxypropyltrimethoxylsilane (GPS, 97%, TCI), tetraethoxysilane (TEOs), ethanol, ammonia, chloroform and other solvents are purchased from Sinopharm Chemical Reagent Co., Ltd. (SCRC) and all of analytical grade without further purification. Hyperbranched poly (ethylene imine) (HPEI, M_n = 10 000) was purchased from Aldrich. 2-(2,3-Epoxypropyloxy) thioxanthone (ETX) was synthesized in our lab according to the procedure described in literature (44). Methyl methacrylate (MMA, from SCRC) was purified by washing with 5% NaOH to remove the inhibitor and then double distillation under reduced pressure; it was then stored in the refrigerator before using. Anhydrous toluene was prepared by drying with anhydrous calcium hydride and then distilling under reduced pressure before using. The PMMA matrix for commercial use with molecular weight (M_w) of 36 000 was provided by BASF.

Synthesis of Hyperbranched Thioxanthone Photoinitiator (HPTX). HPTX was prepared by previously reported methods (44). HPTX was synthesized by incorporating ETX into HPEI. The detail synthesis procedure is as follows. ETX (0.284 g, 1 mmol) and HPEI (0.215 g, 5 mmol in terms of $-CH_2CH_2N-$ repeat unit) were added to ethanol (10 mL), and the mixture was refluxed for 24 h at 80 °C under nitrogen. The solution was then dropped into 10-fold anhydrous ether and filtered to get the product, then dried in a vacuum.

^{1}H NMR ($CDCl_3$): δ 8.58−7.21 (aromatic), 4.10−3.80 ($-OCH_2$, $-OCH$), 3.72−3.40 ($-OCH_2CH_2$), 2.8−2.4 ($-NCH_2CH_2$). FTIR (KBr): 3326 (−OH), 2880 (−CH), 1630 (C═O).

Synthesis and Chemical Modification of Silica Particles. Monodispersed silica particles with different sizes were prepared by hydrolysis of TEOs with ammonia according to the so-called Stöber method (45). One-hundred milliliters of ethanol was added into a single-necked round-bottom flask (500 mL) equipped with a IKA Heat-Up Magnetic Agitator and heated to 40 °C; TEOS (2 mL) was then added into ethanol under magnetic stirring at a speed of 500 rpm. Five minutes later, the mixture of ammonia (4 mL) and ultrapure water (1.5 mL) was added into the flask. The mixture was first stirred at a speed of 800 rpm for 6 min and then at the speed of 500 rpm for 18 h. At last, the SPs with a mean diameter of 200 nm was obtained. The obtained particles were then purified by centrifugation/redispersion three times using ethanol and finally stored in 50 mL of ethanol.

The above-obtained SPs were centrifuged and redispersed in anhydrous toluene for three times, and then redispersed in 50 mL of fresh anhydrous toluene. After heated to 50 °C, 1 mL of 3-glycidoxypropyltrimethoxylsilane (GPS) was quickly injected into the flask. The mixture was stirred at 50 °C for 24 h under dry nitrogen and cooled to room temperature. The GPS-modified silica particles (SiO_2@GPS) were separated by centrifugation at 4000 rpm. After getting rid of the supernatant, the particles were redispersed in toluene and centrifugated again. The above purification cycle was repeated for three times to remove excess GPS. The epoxy-functionalized silica particles (SiO_2@GPS) were finally redispersed in 50 mL of anhydrous toluene.

Immobilization of HPTX. The functionalized silica particles (SiO_2@GPS) were dealt with centrifugation/redispersion for three times using chloroform before the following reaction. Typically, SiO_2@GPS was redispersed in 30 mL of fresh chloroform and 0.15 g of HPTX (concentration = 0.01 mol L^{-1}) was added into the solution. The mixture was refluxed for 24 h under dry nitrogen and then cooled to room temperature. The HPTX-functionalized silica particles (SiO_2@HPTX) were separated by centrifugation, washed in chloroform five times, and dried in vacuo at room temperature for 8 h.

Surface-Initiated Photopolymerization of PMMA from SiO2@HPTX. Photopolymerization was conducted in an oxygen-free environment. Ten milligrams of SiO_2@HPTX and 5 mL of MMA were added into a transparent vial equipped with a magnetic stir bar. The mixture was subjected to three freeze−pump−thaw cycles and then sealed. Photopolymerization was carried out at room temperature and the vial was kept 10 cm away from UV light (λ_{max} = 365 nm). The polymerization was ended by moving the vail out of the UV light. Hybrid particles were isolated via centrifugation at 4000 rpm and the supernatant was collected for some characterizations. Then the particles

were dispersed into 10 mL of tetrahydrofuran (THF) which can remove PMMA absorbed on the particles. The solvent (THF) was replaced every eight hours. Particles were purified by centrifugation/redispersion for three times and then dried at room temperature under a vacuum to generate SiO2@PMMA.

Preparation of PMMA Film Composite Containing SiO2@PMMA Hybrid Particles. SiO_2@PMMA-2 h (0.029 g; raw SPs in hybrid particles accounts for 2 wt % PMMA matrix) and 0.100 g of raw SPs were implanted into 5 g PMMA matrixes using 3 mL of toluene as the solvent. Then well-stirred mixtures were sonicated for 10 min before being cast onto horizontal glass plates. The films first dried in an air oven at 45 °C for 5 h and then dried in vacuo at 120 °C for 48 h to get rid of solvents. The films kept in the vacuum dryer at room temperature before characterizations. Then relatively smooth, flat, and transparent films of uniform thickness(~50 μm) were well-prepared. Meanwhile, pure PMMA was also made into film in a similar way.

CHARACTERIZATION

Gel Permeation Chromatography (GPC). Molecular weights and molecular weight distributions were determined by a gel permeation chromatograph (GPC) on a Perkin-Elmer Series 200 apparatus. THF was used as the eluent at a flow rate of 1.0 mL/min and polystyrene as the calibration standard.

Grafting Density Calculations (D_s). The grafting density in chains per surface area (D_s, chains/nm^2) may be calculated according to eq 1 from the molecular weight (M_n, g/mol), graft amount (W), surface area (S), and Avogadro's number (N_a, molecules/mol).

$$D_s = \frac{WN_a}{M_n S} \quad (1)$$

Fourier Transform Infrared Spectroscopy (FT-IR). Fourier transform infrared (FT-IR) spectra were recorded on a Perkin-Elmer Paragon 1000 FTIR spectrometer. The samples were prepared as KBr disk.

Thermogravimetric Analysis (TGA). TGA was performed in nitrogen at a heating rate of 20 °C/min from 100 to 800 °C using a TA Q5000IR TGA. For each measurement, the sample cell was maintained at 100 °C for 30 min to evaporate the solvent in the sample before measurement.

Differential Scanning Calorimeter (DSC). DSC was performed in nitrogen with a Perkin-Elmer Pyris 1 instrument at a heating rate of 20 °C/min.

Ultraviolet−Visible Spectra. UV−vis spectra were recorded in THF solution by a Shimadzu 2550 UV−vis spectrophotometer (concentration = 0.1 g L^{-1} in terms of raw SPs in all the solutions). All the films were measured directly.

Transmission Electron Microscopy (TEM). TEM observations were conducted on a JEOL 2100F transmisssion electron microscope operating at an acceleration voltage of 200 kV. The sample for TEM observations was prepared by placing a 10 μL particle solution on copper grids successively coated with thin films of carbon. No staining was required.

Scanning Electron Microscopy (SEM). SEM was performed using a JSM-7401F scanning electron microscope at an acceleration voltage of 1 kV or 5 KV. Samples were mounted on silica wafers and those with organic layers were sputtercoated with gold to minimize charging.

Tensile Measurements. Tensile measurements were performed with an Instron 4465 instrument in a N_2 ambient atmosphere at a crosshead speed of 2 mm/min.

RESULTS AND DISCUSSION

Immobilization of Photoinitiator HPTX on SPs. Because of easy preparation and wide applications in many fields such as composite material, template, and photonic crystals (14, 46−48), silica particles are usually chosen as an ideal inorganic core in studies. Monodispersed silica particles can be easily fabricated with tunable sizes from 5 nm to 100 μm in diameter. In this work, silica particles of 200 nm in diameter, as determined by TEM and SEM, were synthesized through the well-known Stöber process (45). The strategy for photochemical synthesis of PMMA brush on SPs is illustrated in Scheme 1. The whole process includes two steps: immobilization of hyperbranched thioxanthone photoinitiator (HPTX) on the surface of SPs and surface-initiated photopolymerization of MMA. In the process of immobilization of HPTX, epoxy groups were first introduced on the surface of SPs by chemical modification of raw SPs using 3-glycidoxy-propyltrimethoxylsilane (GPS). On the basis of the rather efficient nucleophilic addition reaction between epoxy and amino groups, a monolayer of HPTX was able to be readily rooted on the surface of SPs through a covalent bond, which provides an essential prerequisite for surface-initiated photopolymerization (SIPP). The processes for immobilization of photoinitiator were traced by TEM, FT-IR, TGA, UV−vis, and SEM.

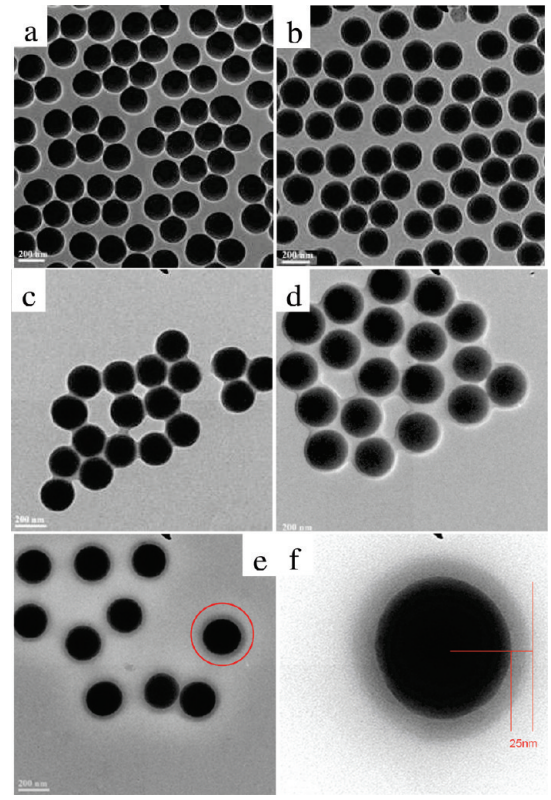

FIGURE 1. TEM images of (a) SiO_2 (raw SPs), (b) SiO_2@GPS, (c) SiO_2@HPTX, (d) SiO_2@PMMA-2 h, (e) SiO_2@PMMA-5 h, (f) SiO_2@PMMA-5 h in high resolution.

TEM images of SPs at different stages are shown in Figure 1. Compared with the raw SPs (SiO_2) and SiO_2@GPS revealed in images a and b in Figure 1, an obvious organic layer can be observed on the SPs in Figure 1c−e. Small molecular GPS modified SPs with smooth surface (SEM, Figure 5b) have no obvious differences in the TEM image (Figure 1b). It is found that hyperbranched polymeric thioxanthone (HPTX) with plenty of amino groups was success-

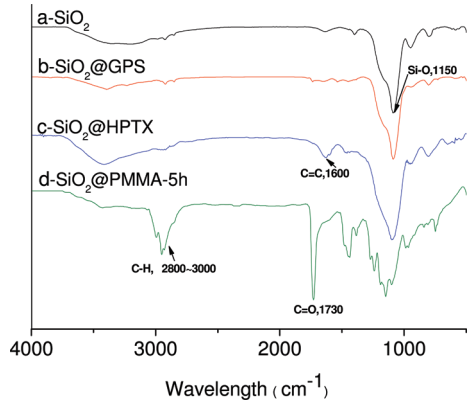

FIGURE 2. FT-IR spectra of (a) SiO_2 (raw SPs), (b) SiO_2@GPS, (c) SiO_2@HPTX, (d) SiO_2@PMMA-5 h.

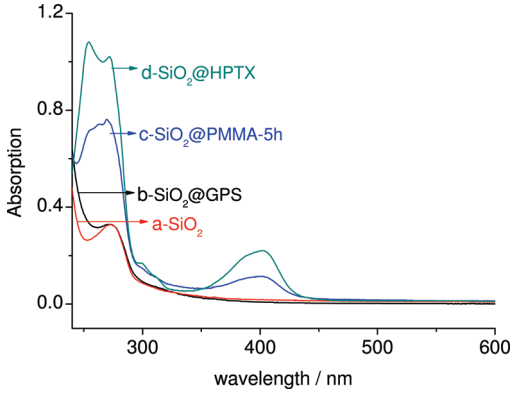

FIGURE 3. UV−vis spectra of (a) SiO_2 (raw SPs), (b) SiO_2@GPS, (c) SiO_2@HPTX, (d) SiO_2@PMMA-5 h in toluene.

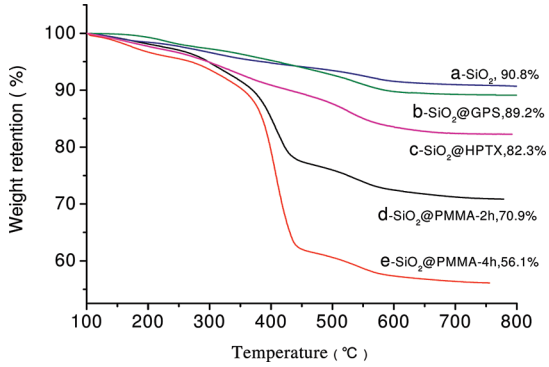

FIGURE 4. TGA of (a) SiO_2 (raw SPs), (b)SiO_2@GPS, (c) SiO_2@HPTX, (d) SiO_2@PMMA-2 h, (e) SiO_2@PMMA-5 h. TGA was performed in air at a heating rate of 20 °C /min.

fully grafted onto the surface of SiO_2@GPS, resulting in the obvious organic layer (~3 nm) shown in TEM graph (Figure 1c). The obtained photoinitiator HPTX functionalized SPs (SiO_2@HPTX) were further confirmed by FT-IR (Figure 2), UV−vis (Figure 3), TGA (Figure 4) and SEM (Figure 5c). As a comparison to the FT-IR spectra of raw SPs (SiO_2) and SiO_2@GPS (Figure 2a,b), the appearance of the absorbance band at 1640 cm^{-1} in Figure 2c was characteristic of C═O vibrations for thioxanthone moieties of HPTX. SiO_2@HPTX exhibits the absorption maximum around 400 nm, which is the characteristic UV−vis absorption of thioxanthone (Figure 3). The little bigger SiO_2@HPTX shown in the SEM image (Figure 5) was also in support of our conclusion. All

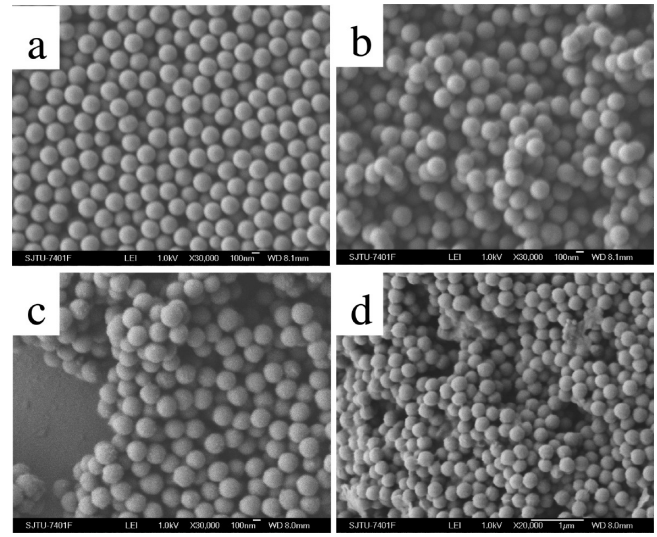

FIGURE 5. SEM images of (a) SiO_2 (raw SPs), (b)SiO_2@GPS, (c) SiO_2@HPTX, (d) SiO_2@PMMA-5 h.

these results are the best evidence to confirm the successful attachment of HPTX on SPs. The amount of HPTX on the surface of SPs can be further determined by TGA analysis. In Figure 4, the weight retentions at 800 °C were 90.8 % for raw SPs, 89.2 % for SiO_2@GPS, and 82.3 % for SiO_2@HPTX. The weight loss of raw SPs might be caused by associated water loss and continued condensation. In the weight retention at 800 °C, there exists a 1.6 % difference between raw SPs and SiO_2@GPS, and 6.9 % difference between SiO_2@GPS and SiO_2@HPTX. We can roughly estimate that the densities of GPS and HPTX on the particles' surface are, respectively, 4.7 and 0.16 molecule/nm^2 according to eq 1.

Photochemical Synthesis of PMMA Brush on SPs. PMMA brush on SPs (SiO_2@PMMA) was synthesized through surface-initiated photopolymerization (SIPP) using a high-pressure Hg lamp as the UV light source. In the presence of co-initiator amino groups, the photolysis of thioxanthone can lead to formation of an radical produced from TX (ketyl radical) and another radical derived from the hydrogen donor amine. The polymerization of MMA is usually initiated by amino radicals, and the ketyl radicals are not active because of steric hindrance. Because TX moieties of HPTX were photobleached to generate ketyl radicals, the UV absorption of TX at 400 nm in Figure 3d decreased after UV light exposure. The morphology of the obtained SiO_2@PMMA hybrid particles were revealed by TEM (Figure 1d−f). According to Figure 1, well-defined PMMA brush on SPs was successfully synthesized through SIPP. With the increase in exposure time, the PMMA brush layer became thicker (Figures 1d and 1e). After photopolymerization for 5 h, the mean thickness of PMMA brush layers is about 25 nm and the diameter of SiO_2@PMMA-5 h is about 250 nm according to images of TEM and SEM (Figures 1e, 1f, and 5d). The formation of PMMA brush layer can be further confirmed by FT-IR and TGA. Compared with FT-IR spectra of SiO_2@HPTX in Figure 2c, the appearance of peak at 1720 cm^{-1} derived from C═O of PMMA in Figure 2d, indicated the successful formation of PMMA brush on SPs. The amount

Table 1. Data of the PMMA Brush on SPs by Surface-Initiated Photopolymerization[a]

sample	weight loss[b] (%)	$M_n \times 10^{-5}$[c]	M_w/M_n[c]	graft density (D_s) (chains/nm^2)
raw SiO_2	90.8			
SiO_2@ GPS	89.2			4.7
SiO_2@ HPTX	82.3			0.16
SiO_2@ PMMA-1 h	75.4	1.68	1.4	0.016
SiO_2@ PMMA-2 h	70.9	1.67	1.6	0.030
SiO_2@ PMMA-3 h	62.6	1.69	1.4	0.045
SiO_2@ PMMA-4 h	56.1	2.03	1.2	0.058
SiO_2@ PMMA-5 h	48.5	2.51	1.5	0.071

[a] Bulk polymerization of MMA; light intensity is about 6.5mw/cm^2. [b] Determined by TGA. [c] Determined by GPC; THF was used as the eluent and PS as standard.

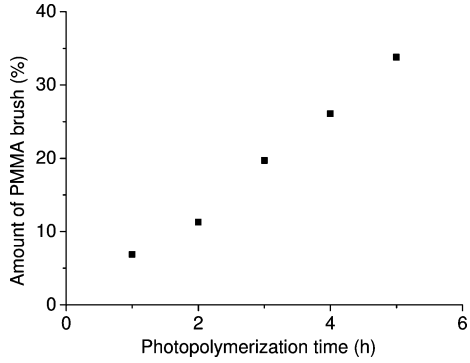

FIGURE 6. Amount of PMMA Brush Layer vs Photopolymerization Time.

of PMMA brush layer can be determined by TGA (Figure 4), and the detailed amount of PMMA brush layer at different exposure times is summarized in Table 1. According to Figure 4 and Table 1, the amount of PMMA brush layer increases with the photopolymerization time. If the density of the PMMA organic layer is about 1.04 g/cm^3, the PMMA thickness of SiO_2@PMMA-5 h can be estimated to be 23 nm based on the data of TGA, which is in good agreement with TEM results (25 nm). The amount of PMMA layer determined by TGA vs photopolymerization time is shown in Figure 6, which indicates that the amount of PMMA brush layer can be well-controlled by photopolymerization time. This also means the thickness of PMMA brush layers of SiO_2@PMMA hybrid particles is tunable.

Because of chain transfer in the photopolymerization of MMA, the free PMMA can be generated in the solution besides PMMA brush attached on the surface of silica particles. The molecular weight (M_n) and polydispersity of the free PMMA in solution were checked by GPC, which can be considered to be the similar to those of PMMA brush on the substrate (49, 50). The M_n of PMMA is about 1.7×10^5 for first 3 h of exposure time, and increases to above 2.0×10^5 when exposure time increases to 4 h. This might be attributed to lightly cross-linked reaction of PMMA chain under UV light exposure for longer time. On the basis of the amount of PMMA brush layers determined by TGA and M_n derived from GPC, the graft density of PMMA can be estimated, and these results are summarized in Table 1.

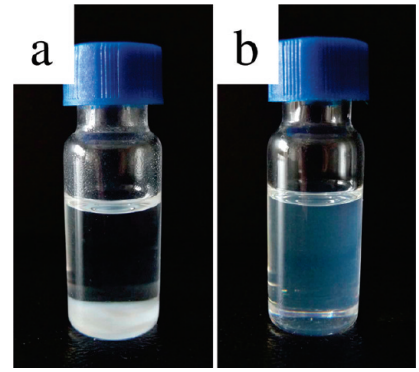

FIGURE 7. Photopictures of (a) SiO_2 and (b) SiO_2@PMMA-5 h in toluene.

Table 2. Thermal and Mechanical Properties of PMMA Composite, Raw SP Content is 2%

sample	T_g (°C)	T_d (°C)	max stress (MPa)	modulus (MPa)
pure PMMA	82.2	383.2	27.3	1495
PMMA-SiO_2	84.3	385.0	29.5	1775
PMMA-SiO_2@PMMA-5 h	89.6	393.5	37.6	2033

Figure 7 shows the pictures of disperse property of the raw SPs and SiO_2@PMMA-5 h in toluene. Compared with the raw SPs, the obtained SiO_2@PMMA-5 h hybrid particles can be better dispersed in toluene, and the resulting solution is stable for more than 1 day. The good dispersion of SiO_2@PMMA hybrid particles in toluene should be attributed to the good solubility of PMMA brush layer in organic solvent, which is a key factor in fabrication of SiO_2@PMMA composite film.

PMMA Composite Containing SiO_2@PMMA Hybrid Particles. Polymer−matrix composites represent a series of attractive characters compared to conventional pure polymer materials (51, 52). As there's interface between the organic and inorganic phases, SiO2@PMMA hybrid particles were expected to improve thermal and mechanical properties of PMMA composite better than raw SPs.

By adding 2 wt % raw SPs and SiO_2@PMMA hybrid particles into PMMA matrixes, PMMA-raw SPs and PMMA-SiO_2@PMMA composite films were prepared. The thermal and mechanical properties of PMMA-raw SiO_2 and PMMA-SiO_2@PMMA composites carefully measured more than five times with pure PMMA for comparison were summarized in Table 2. Compared with pure PMMA and PMMA-raw SiO_2, the glass-transition temperature (T_g) of PMMA-SiO2@PMMA increases about 7.4 and 5.3 °C, respectively. Similarly, decomposition temperature (T_d) of PMMA-SiO_2@PMMA is the highest among these three samples. Compared with pure PMMA, the maximum stress and young's modulus of PMMA-SiO_2@PMMA increased from 27.3 to 37.6 MPa, and from 1495 to 2033 MPa, respectively. The maximum stress and young's modulus of the PMMA-SiO_2@PMMA composite were respectively increased by 25 and 15%, in comparison to PMMA-raw SiO_2. Because of the well-defined PMMA brush layer outside of SPs, SiO_2@PMMA is expected to possess good compatibility with the PMMA matrix, resulting in low

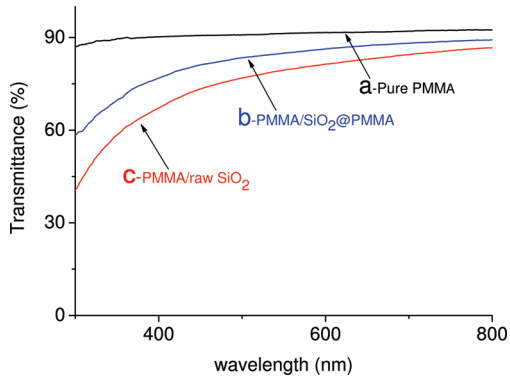

FIGURE 8. UV−vis spectra of (a) pure PMMA film, (b) PMMA film containing SiO_2@PMMA hybrid particles, (c) PMMA film containing raw SPs. Raw SP content is 2%.

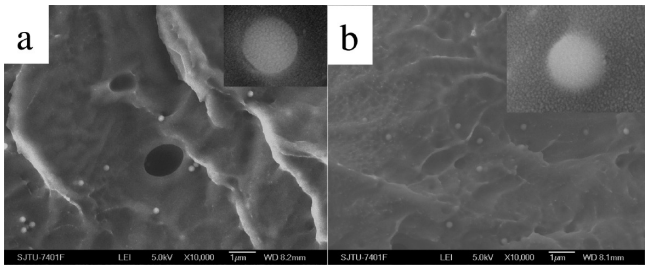

FIGURE 9. SEM images of fractured surface: (a) PMMA composite films containing raw SiO_2 particles, (b) PMMA composite films containing SiO_2@PMMA-5 h hybrid particles. Raw SP content is 2%.

interface energy between hybrid particles and matrix that might lead to the enhanced thermal and mechanical properties of composite films.

All the enhanced thermal and mechanical properties can be explained by the SEM images (Figure 9) that separately display the fractured surfaces of PMMA composites with raw silica particles and SiO_2@PMMA hybrid particles. Though either mechanical or thermal properties of PMMA hybrid films with raw SPs show certain improvements, we can still observe the distinct interfaces between raw SPs and PMMA matrix. In contrast, SiO_2@PMMA hybrid particles absolutely blend in the surrounding PMMA matrix, which led to substantial improvements in a variety of properties.

PMMA has several desirable properties, of which exceptional optical clarity is the most attractive. The UV−vis spectra of the obtained PMMA composite and pure PMMA films are shown in Figure 8. The optical clarity of pure PMMA films shows more than 90% optical transmission during most of UV−vis wavelength range (i.e., 700 to 300 nm). By incorporation of SiO_2@PMMA hybrid particles, the optical clarity of PMMA-SiO_2@PMMA films exhibits a slight decrease, but still rather better than PMMA-raw SiO_2. Indeed, it is evident enough to distinguish them by the unaided eye in the preparation of composite samples.

CONCLUSION

The PMMA brush on SPs (hybrid particles) was fabricated through a novel and reliable strategy by combination of immobilization of hyperbranched polymeric thioxanthone (HPTX) on the surface and surface-initiated photopolymerization (SIPP). The thickness of PMMA brush layers increases with the increase of exposure time of UV-light, and reaches about 25 nm after 5 h exposure. The obtained SiO_2@PMMA hybrid particles can be implanted into the PMMA matrix to lead to a PMMA composite with enhanced thermal and mechanical properties.

Acknowledgment. The authors express their gratitude to National Natural Science Foundation of China (50803036) and Science & Technology Commission of Shanghai Municiple Government (08520704700) for their financial support.

REFERENCES AND NOTES

(1) Milner, S. T. *Science* **1991**, *251*, 905.
(2) Feng, J. X.; Haasch, R. T.; Dyer, D. J. *Macromolecules* **2004**, *37*, 9525.
(3) Jiang, X. M.; Wang, B. B.; Li, C. Y.; Zhao, B. *J. Polym. Sci., Part A: Ploym. Chem.* **2009**, *47*, 2853.
(4) Ranjan, R.; Brittain, W. J. *Macromol. Rapid Commun.* **2008**, *29*, 1104.
(5) Wei, B.; Gurr, P. A.; Gozen, A. O.; Blencowe, A.; Solomon, D. H.; Qiao, G. G.; Spontak, R. J.; Genzer, J. *Nano Lett.* **2008**, *8*, 3010.
(6) Hensarling, R. M.; Doughty, V. A.; Chan, J. W.; Patton, D. L. *J. Am. Chem. Soc.* **2009**, *131*, 14673.
(7) Rider, D. A.; Chen, J. I. L.; Eloi, J.-C.; Arsenault, A. C.; Russell, T. P.; Ozin, G. A.; Manners, L. *Macromolecules* **2008**, *41*, 2250.
(8) Norder, W.; Gage, D. *Langmiur* **2004**, *20*, 4162.
(9) Lahiri, J.; Isaacs, L.; Grzybowski, B.; Carbeck, J. D.; Whitesides, G. M. *Langmiur* **1999**, *15*, 7186.
(10) Hucknall, A.; Rangarajan, S.; Chilkoti, A. *Adv. Mater.* **2009**, *21*, 2441.
(11) Kataoka, D. E.; Trolan, S. M. *Nature* **1999**, *402*, 794.
(12) Zhao, B.; Brittain, W. J. *Prog. Polym. Sci.* **2000**, *25*, 677.
(13) Park, J. W.; Thomas, E. L. *J. Am. Chem. Soc.* **2002**, *124*, 514.
(14) Morinaga, T.; Ohkara, M.; Ohno, K.; Tsujii, Y.; Fukuda, T. *Macromolecules* **2007**, *40*, 1159.
(15) Chen, R.; Zhu, S.; Maclaughlin, S. *Langmiur* **2008**, *24*, 6889.
(16) Zhou, L.; Gao, C.; Xu, W. J.; Wang, X.; Xu, Y. H. *Biomacromolecules* **2009**, *10*, 1865.
(17) Kaholek, M.; Lee, W. K.; Feng, J.; LaMattina, B.; Dyer, D. J.; Zauscher, S. *Chem. Mater.* **2006**, *18*, 3660.
(18) Beinhoff, M.; Frommer, J.; Carter, K. R. *Chem. Mater.* **2006**, *18*, 3425.
(19) Schmidt, R.; Zhao, T.; Green, J. B.; Dyer, D. J. *Langmuir* **2002**, *18*, 1281.
(20) Ohno, K.; Morinaga, T.; Koh, K.; Tsujii, Y.; Fukuda, T *Macromolecules* **2005**, *38* (6), 2137.
(21) Cheng, C.; Khoshdel, E.; Wooley, K. L. *Nano Lett.* **2006**, *6*, 1741.
(22) Khire, V. S.; Harant, A. W.; Watkins, A. W.; Anseth, K. S.; Bowman, C. N. *Macromolecules* **2006**, *39*, 5081.
(23) Rowe, M. D.; Hammer, B. A. G.; Boyes, S. G. *Macromolecules* **2008**, *41*, 4117.
(24) Liu, J. Q.; Yang, W. R.; Zarele, H. M.; Gooding, J. J.; Paris, T. P. *Macromolecules* **2009**, *42*, 1931.
(25) Morandi, G.; Pascual, S.; Montembault, V.; Legoupy, S.; Delorme, N.; Fontaine, L. *Macromolecules* **2009**, *42*, 6927.
(26) Weck, M.; Jackiw, J. J.; Rossi, R. R.; Weiss, P. S.; Grubbs, R. H. *J. Am. Chem. Soc.* **1999**, *121*, 4088.
(27) Feng, J.; Haasch, R. T.; Dyer, D. J. *Macromolecules* **2004**, *37*, 9525.
(28) Kaholek, M.; Lee, W. K.; Feng, J.; Mattina, B. L.; Dyer, D. J.; Zauscher, S. *Chem. Mater.* **2006**, *18*, 3660.
(29) Steenackers, M.; Kuller, A.; Stocheva, S.; Grunze, M.; Jordan, R. *Langmiur* **2009**, *25*, 2225.
(30) Ionov, L.; Minko, S.; Stamm, M.; Gohy, J. F.; Jrme, R.; Scholl, A. *J. Am. Chem. Soc.* **2003**, *125*, 8302.

(31) Satoh, M.; Shirai, K.; Saitoh, H.; Yamauchi, T.; Tsubokawa, N. *J. Polym. Sci.: Part A: Ploym. Chem.* **2005**, *43*, 600.
(32) Imroz Ali, A. M.; Mayes, A. G. *Macromolecules* **2010**, *43*, 837.
(33) Yoshikawa, C.; Goto, A.; Tsujii, Y.; Fukuda, T.; Yamamoto, K.; Kishida, A. *Macromolecules* **2005**, *38*, 4604.
(34) Schmidt, R.; Zhao, T.; Green, J. B.; Dyer, D. J. *Langmuir* **2002**, *18*, 1281.
(35) Dyer, D. J.; Feng, J.; Schmidt, R.; Wong, V. N.; Zhao, T.; Yagci, Y. *Macromolecules* **2004**, *37*, 7072.
(36) kishimoto, K.; Suzawa, T.; Yakata, T.; Mukai, T.; Ohno, H.; kato, T. *J. Am. Chem. Soc.* **2005**, *127*, 15618.
(37) Mateo, J. L.; Serrano, J.; Bosch, P. *Macromolecules* **1997**, *30*, 1285.
(38) Jia, X. Y.; Jiang, X. S.; Liu, R.; Yin, J. *Macromol. Chem. Phys.* **2009**, *210*, 1876.
(39) Jiang, X. S.; Yin, J. *Chem. Commun.* **2005**, 4927.
(40) Jiang, X. S.; Yin, J. *Macromolecules* **2004**, *37*, 7850.
(41) Green, A. W.; Timms, A. W.; Green, P. N. In *Proceedings of Radtech Europe '91*; Edinburgh, Scotland, Sept 29—Oct 2, 1991; RadTech Europe: Fribourg, Switzerland, 1991; p 636.
(42) LouieM. W.; Liu, H. W.; Lam, M. H.-C.; Lau, T.-C.; Lo K., K.-W. *Organometallics,* **2009**, *28*, 4297.
(43) Angiolini, L.; Caretti, D.; Corelli, E.; Carlini, C. *J. Appl. Polym. Sci.* **1995**, *55*, 1477.
(44) Wen, Y. S.; Jiang, X. S.; Liu, R.; Yin, J. *Polymer* **2009**, *50*, 3917.
(45) Stöber, W.; Fink, A. *J. Colloid Interface Sci.* **1968**, *26*, 62.
(46) Gao, D.; Zhang, Z. Q.; Wu, M. H.; Xie, C. G.; Guan, G. J.; Wang, D. P. *J. Am. Chem. Soc.* **2007**, *129*, 7859.
(47) Ge, J; Lee, H.; He, L.; Kim, J.; Lu, Z.; Kim, H.; Goebl, J.; Kwon, S.; Yin, Y. *J. Am. Chem. Soc.* **2009**, *131*, 15687.
(48) Wang, H. L.; Shi, T. J.; Yang, S. Z.; Zhai, L F.; Hang, G. P. *J. Appl. Polym. Sci.* **2005**, *101*, 810.
(49) Baum, M.; Brittain, W. J. *Macromolecules* **2002**, *35*, 610.
(50) Brinks, M. K.; Studer, A. *Macromol. Rapid Commun.* **2009**, *30*, 1043.
(51) Kuo, M. C.; Tsai, C. M.; Huang, J. C.; Chen, M. *Mater. Chem. Phys.* **2005**, *90*, 185.
(52) Yeh, J. M.; Huang, K. Y.; Dai, C. F.; Chand, B. G.; Weng, C. J. *J. Appl. Polym. Sci.* **2008**, *110*, 2108.

AM900758J